Nonlinear Filter Design for Pose and IMU Bias Estimation

Glauco Garcia Scandaroli, Pascal Morin.

INRIA Sophia Antipolis-Méditerranée
2004 route des Lucioles, Sophia Antipolis 06902, France.
Glauco.Scandaroli@inria.fr, Pascal.Morin@inria.fr

***Abstract*— This paper concerns the problem of position and attitude estimation based on the fusion of complementary sensors. Nonlinear observers are proposed in order to obtain high-quality and high-rate estimates from raw position/attitude data, and measurements obtained from an inertial measurement unit. Estimates are improved through the online identification of diverse measurement biases, and a novel method for concurrent position estimation and accelerometer bias estimation is presented. *Almost* global asymptotic convergence of the pose observer is proved based on a Lyapunov-like approach, and several implementation issues are addressed. Comparison with classical existing methods illustrate the relevance of the proposed approach.**

***Index Terms*— Inertial Estimation, Nonlinear Observers, Lyapunov Function.**

I. Introduction

This work deals with pose (i.e. position and attitude) estimation via the fusion of sensory measurements. Given pose and inertial measurements, the objective is to obtain estimates that best exploit the different measurements characteristics, while coping with measurements biases. This issue is fundamental in ground or aerial robotic applications, where a precise knowledge of the robot location is often required. In general, high frequency measurements, typically from 50 Hz up to 1 kHz, of rotational velocity and specific translational acceleration are provided by an inertial measurement unit (IMU). As a result of micro-electro-mechanical sensors (MEMS) manufacturing characteristics, IMU measurements are corrupted by additive noise and offset, also known as measurement bias. Therefore, the solution of such problem using solely IMU data integration drifts after a few seconds. The reduction of such drift can be achieved after a good calibration of sensor's bias, still, the time invariant model for bias is only an approximation, additionally it does not consider effects from temperature variation. Therefore, the consideration of an online method for bias estimation is indeed positive. Other sensors, that provide explicit or implicit attitude and position measurements, must be employed in order to cope with the calibration, and bound the resulting drift from IMU data integration. Examples are given by the global positioning system (GPS) and/or visual sensors. These sensors can provide a fair measurement of position, however at low frequencies, typically from 5 Hz up to 25 Hz. GPS provides position with respect to earth, or to a ground fixed station for differential GPS. However, this system needs a direct sight to the satellites (or to the stations), therefore it is not suitable for several types of environments. Visual systems are able to relate the rotation and translational displacement from two different views, thus providing incremental measurements.

Since early works on attitude estimation, the extended Kalman filter (EKF) is the incipient solution to this estimation problem [1]. However, EKF provides no assurance of convergence, which can be seen from its similarity to the first step of Gauss-Newton optimization method [2]. Other Kalman-based solutions have been proposed to overcome the nonlinear nature of the problem [3], [4]. Despite the fact that these methods improve significantly the propagation of the probability distribution, up to the authors knowledge, the achievement of *almost* global convergence using such methods remains to be achieved. To overcome such nonlinear propagation of the distribution the use of uncertainty ellipsoids [5] have been proposed in the literature. Additionally, the problem can be rewritten as estimation of two non-collinear unconstrained vectors instead of the attitude matrix or some parametrization, hence becoming a linear time-varying system estimation problem [6].

In the past years, some effort has been put in the development of nonlinear observers for attitude, attitude-heading reference (AHR) and pose estimation. Nonlinear observers are application-specific estimators that take advantage of structural properties of the models. Although some technical differences can be noticed between different nonlinear observers, this class of estimators commonly share the benefits of global, or at least semi-global, stability proofs. Some state-of-the-art results are Lyapunov-function based observers [7]–[9], complementary filters for $\mathbf{SO}(3)$ [10], and invariant-observers [11], [12]. Concerning online bias estimation, an AHR estimator that accomplishes gyroscope and (partial) accelerometer bias estimation is presented in [12].

In order to solve the full pose estimation using nonlinear observers, the decoupling of the attitude and translational displacement is often considered. An observer for attitude and position using inertial data and visual line features, is presented in [13], despite the fact that biases are considered for the presented simulation results, there is no procedure for bias estimation in the observer. The estimation using the $\mathbf{SE}(3)$ representation by means of IMU and bearing measurements is addressed in [14], but online IMU bias estimation is not performed. A cascaded nonlinear observer for attitude and position is presented in [15] exploiting

G. G. Scandaroli is funded by grants from the *Conseil Régional Provence-Alpes-Côte d'Azur*, and the *DGCIS* Rapace project leaded by Geocean.

IMU measurements together with GPS measurements. Exponential convergence for attitude and position is achieved, together with gyroscope bias estimation. Cheviron *et. al* [16] presents a solution for full pose estimation, however due to misconceived hypothesis on the accelerometer measurement definition the convergence proof for position estimation is only valid for small angular velocities.

This paper presents the development of a nonlinear observer that employs the passive complementary filter for attitude estimation, and a novel method for concurrent position and accelerometer bias estimation. While the present approach bears resemblance with [16], in the sense that a position and accelerometer bias observer is presented, the observer form is different due to the definition of the system. This article also presents a global exponential stability proof for the position and accelerometer bias observer independently of the angular velocity, and *almost* global asymptotic stability for the nonlinear pose and IMU bias observer. Recall that, due to a topological obstruction, global stability on $\mathbf{SO}(3)$ cannot be achieved. A method for gain tuning based on settling time estimates is also presented. In addition to the guarantee of *almost* global convergence, the implementation of the proposed method is simpler than Kalman-based estimators. Simulation results illustrate the performance of the method, and a comparison with the EKF is presented. While the simulations are developed using inertial and visual data, the proposed method can be used with any measurement system that is able to recover attitude and position.

II. Background

A. Mathematical Notation and Identities

The special orthogonal group is denoted as $\mathbf{SO}(3)$. Its associated Lie algebra is the set of anti-symmetric matrices denoted as $\mathfrak{so}(3)$. For the sake of design and analysis, the following properties and definitions are recalled from [10]. The cross-product can be represented by the product $S(u)v = u \times v,\ \forall\ u, v \in \mathbb{R}^3$, where $S(\cdot) \in \mathfrak{so}(3)$. The inverse of the $S(\cdot)$ operator is denoted $\mathbf{vex}(\cdot)$, i.e., $\mathbf{vex}(S(u)) = u,\ u \in \mathbb{R}^3,\ S(\mathbf{vex}(A)) = A,\ A \in \mathfrak{so}(3)$. With $A \in \mathbb{R}^{3\times 3}$, the symmetric and anti-symmetric operators are defined as $\mathbf{P_s}(A) = \frac{A+A^T}{2}$, $\mathbf{P_a}(A) = \frac{A-A^T}{2}$. The following properties hold:

$$\begin{aligned} S(Ru) &= RS(u)R^T, \quad u \in \mathbb{R}^3, R \in \mathbf{SO}(3), \\ R\ \mathbf{vex}\big(\mathbf{P_a}(R)\big) &= \mathbf{vex}\big(\mathbf{P_a}(R)\big), \qquad R \in \mathbf{SO}(3)\,. \end{aligned} \tag{1}$$

At a few places in this paper, parametrizations of $\mathbf{SO}(3)$ will be used, and willing further information the interested reader is conducted to [17]. Consider any parametrization Θ such that $R \approx I_3 + S(\Theta)$ at first order around the 3×3 identity matrix I_3. Examples are given by $\Theta = [\phi, \theta, \psi]^T$, the vector of roll, pitch and yaw Euler angles, or $\Theta = 2q_v$ with q_v the vector part of the unitary quaternion representation. From the general rotation dynamics $\frac{d}{dt}R = RS(u)$, it follows that around $R = I_3$,

$$\tfrac{d}{dt}\Theta \approx u, \qquad \mathbf{vex}\big(\mathbf{P_a}(R)\big) \approx \Theta \tag{2}$$

B. System description

Denote by $\{I\}$ an inertial frame defined as appropriate. Coordinates of a vector expressed in this frame are written with the subscript $\mathcal{I}$. Similarly,$\{\mathcal{B}\}$ denotes a frame attached to a target rigid body, and coordinates of a vector expressed in this frame are written with the subscript $\mathcal{B}$. The attitude is defined as the rotation matrix $R \in \mathbf{SO}(3) : \{\mathcal{B}\} \to \{\mathcal{I}\}$, and the current position $p_{\mathcal{B}}^{\mathcal{I}} \in \mathbb{R}^3$ as the translational displacement of $\{\mathcal{B}\}$ in $\{\mathcal{I}\}$ coordinates. Throughout the text, $p_{\mathcal{B}}^{\mathcal{I}}$ is referred as p for only the displacement of $\{\mathcal{B}\}$ in inertial coordinates is considered. The dynamics for the system comprising attitude and translational displacement writes

$$\tfrac{d}{dt}R = RS(\omega_{\mathcal{B}}), \quad \tfrac{d}{dt}p = v, \quad \tfrac{d}{dt}v = a_{\mathcal{I}} = Ra_{\mathcal{B}}, \tag{3}$$

where $v \in \mathbb{R}^3$ is velocity of the body in inertial coordinates; $\omega_{\mathcal{B}} \in \mathbb{R}^3$, $a_{\mathcal{B}} \in \mathbb{R}^3$ are the rotational velocity and translational acceleration in body coordinates, and $a_{\mathcal{I}} \in \mathbb{R}^3$ is the translational acceleration represented in inertial coordinates.

Assumption 1 *There exist three positive constants $\overline{c}_a$, $\overline{c}_v$, and $\overline{c}_\omega$ such that $\forall t \in [0, \infty)$: $|\omega_{\mathcal{B}}(t)| \leq \overline{c}_\omega$,$|a_{\mathcal{B}}(t)| \leq \overline{c}_a$,$|\ddot{v}(t)| \leq \overline{c}_v$.*

This assumption indicates that the body rotational velocity is bounded, also the body acceleration and its first order time-derivative are bounded. This technical assumption is not restrictive for applications, all the more that the upper bounds $\overline{c}_a$, and $\overline{c}_v$ are not used in the observer's design.

For the sake of rotational velocity and translational acceleration measurement, an IMU consisting of rate gyroscopes and accelerometers is employed, and without loss of generality it is assumed that the IMU reference frame and $\{\mathcal{B}\}$ coincide. Gyroscopes measure the angular velocity $\omega_{\mathcal{B}}$, and accelerometers measure the *specific translational acceleration*, which is the expression of the body's acceleration minus the gravity field in body coordinates. Therefore, effects arisen from the real body acceleration $a_{\mathcal{B}}$ and earth's gravitational field are measured as if they were the same force.

Due to manufacturing characteristics of MEMS, the measurement is modeled as being disturbed by an offset measurement, also called bias. The considered measurement model is often employed

$$\omega = \omega_{\mathcal{B}} + \omega_b, \qquad \tfrac{d}{dt}\omega_b = 0, \tag{4}$$

$$a = R^T\left(\tfrac{d}{dt}v - g_{\mathcal{I}}\right) + a_b, \qquad \tfrac{d}{dt}a_b = 0, \tag{5}$$

where ω, a denote the rate gyroscope and accelerometer measurements; ω_b, a_b denote gyroscope, accelerometer bias, respectively; and $g_{\mathcal{I}}$ is the gravitational acceleration field represented in inertial coordinates. For the previous models, it is important to notice that other sensor characteristics are neglected, such as limited bandwidth and bias variation with respect to temperature and time. Moreover, MEMS measurements are corrupted by an additive measurement noise. These effects are neglected for the observer design. However, these noises are indeed considered for the presented simulations.

The introduced solution assumes position and attitude measurements/estimates. Many methods can be used. For

example, position can be directly measured by a GPS. Attitude is usually more difficult to obtain and its estimation is still a research topic, especially for IMU-magnetometer based solutions [9], [12]. An interesting alternative is vision, since efficient methods are now available to estimate relative displacements in both position and orientation from visual data (see, e.g. [18]). In this work, a camera observing a known target is used to obtain the complete pose.

III. Observer design

In the previous section, the dynamics of the rigid body's pose and the available measurements were defined. In a complete form, considering the actual IMU measurement and Eqs. (3), (4), and (5), then the dynamics of attitude, position, and sensor bias is given by

$$\begin{cases} \frac{d}{dt}R = RS(\omega-\omega_b), & \frac{d}{dt}\omega_b = 0, \\ \frac{d}{dt}p = v, \quad \frac{d}{dt}v = g_{\mathcal{I}} + R(a-a_b), & \frac{d}{dt}a_b = 0. \end{cases} \tag{6}$$

The following observers are defined:

$$\frac{d}{dt}\widehat{R} = \widehat{R}S(\omega-\widehat{\omega}_b+\alpha_R), \qquad \frac{d}{dt}\widehat{\omega}_b = \alpha_\omega, \tag{7}$$

for the attitude, and

$$\frac{d}{dt}\widehat{p} = \widehat{v}+\alpha_p, \ \frac{d}{dt}\widehat{v} = g_{\mathcal{I}} + R(a-\widehat{a}_b)+\alpha_v, \ \frac{d}{dt}\widehat{a}_b = \alpha_a, \tag{8}$$

for position, where $\alpha_R, \alpha_\omega, \alpha_p, \alpha_v, \alpha_a$ are innovation terms defined further on. The estimation errors are defined

$$\widetilde{R} \triangleq R\widehat{R}^T, \quad \widetilde{\omega}_b \triangleq \omega_b - \widehat{\omega}_b, \tag{9}$$

$$\widetilde{p} \triangleq p-\widehat{p}, \quad \widetilde{v} \triangleq v-\widehat{v}, \quad \widetilde{a}_b \triangleq a_b - \widehat{a}_b, \tag{10}$$

then, the estimation error dynamics yields

$$\frac{d}{dt}\widetilde{R} = \widetilde{R}S(-\widehat{R}\widetilde{\omega}_b - \widehat{R}\alpha_R), \qquad \frac{d}{dt}\widetilde{\omega}_b = -\alpha_\omega, \tag{11}$$

$$\frac{d}{dt}\widetilde{p} = \widetilde{v}-\alpha_p, \ \frac{d}{dt}\widetilde{v} = -R\widetilde{a}_b - \alpha_v, \qquad \frac{d}{dt}\widetilde{a}_b = -\alpha_a. \tag{12}$$

The objective of the nonlinear observer's design is to define α_R, α_ω, α_p, α_v, and α_a so that $(\widetilde{R},\widetilde{\omega}_b,\widetilde{p},\widetilde{v},\widetilde{a}_b) = (I_3,0,0,0,0)$ is an asymptotically stable equilibrium of this estimation error dynamics.

Nonlinear observer solutions with semi-global stability have already been proposed in the literature for attitude and online gyroscope bias estimation. One of them is the passive complementary filter on $\mathbf{SO}(3)$ [10].

Lemma 1 ***(Passive complementary filter on*** $\mathbf{SO}(3)$***)*** *Let*

$$\alpha_R = k_1\widehat{R}^T\mathbf{vex}\big(\mathbf{P_a}(\widetilde{R})\big), \ \alpha_\omega = -k_2\widehat{R}^T\mathbf{vex}\big(\mathbf{P_a}(\widetilde{R})\big) \tag{13}$$

with $k_1, k_2 > 0$. Then, for the attitude estimation error dynamics (11)*, the following statements hold:*
1) All solutions converge to $\mathbb{E}_s \cup \mathbb{E}_u$ with $\mathbb{E}_s = (I_3, 0)$, $\mathbb{E}_u = \Big\{(\widetilde{R},\widetilde{\omega}_b) \mid \mathbf{tr}\big(\widetilde{R}\big) = -1\Big\}$.
2) The equilibrium point $(\widetilde{R},\widetilde{\omega}_b) = (I_3, 0)$ is locally exponentially stable.

Remark that observer (7), (13) is the same as the one in [10], despite the different definition of $\widetilde{R}$. This observer is endowed with additional stability properties (see [10] for the complete statement).

The following result concerns the problem of position, and online accelerometer bias estimation. This is the main result of this section and complements Lemma 1.

Theorem 1 ***(Position and accelerometer bias observer)*** *Let*

$$\alpha_p = k_3\widetilde{p}, \quad \alpha_v = k_4\widetilde{p}, \quad \alpha_a = -k_5(I_3+\tfrac{1}{k_3}S(\omega_{\mathcal{B}}))R^T\widetilde{p} \tag{14}$$

with $k_3, k_4, k_5 > 0$ such that $k_5 < k_3k_4$. Then, $(\widetilde{p},\widetilde{v},\widetilde{a}_b) = (0,0,0)$ is a globally exponentially stable equilibrium point of the position estimation error dynamics (12)*.*

Proof. Appendix A.

This theorem provides a globally exponentially stable observer for the position, velocity and accelerometer bias estimation problem, independently of the rotational dynamics. Note that the stability conditions on the gain parameters are necessary. For example, when $\omega_{\mathcal{B}} = 0$, the dynamics of the estimation error is linear and autonomous. Therefore, the gain conditions in Theorem 1 correspond exactly to the stability conditions of this linear system.

It is implicitly assumed in (14) that $\omega_{\mathcal{B}} = \omega - \omega_b$ is directly available to measurements/estimation. In practice, this term should be replaced by the estimate $\omega - \widehat{\omega}_b$, with $\widehat{\omega}_b$ being the output of the attitude observer (7). The following result, derived from Theorem 1, shows that this can be done without consequence on the convergence of the observer.

Corollary 1 *Let*

$$\alpha_p = k_3\widetilde{p}, \ \alpha_v = k_4\widetilde{p}, \ \alpha_a = -k_5(I_3+\tfrac{1}{k_3}S(\omega-\widehat{\omega}_b))R^T\widetilde{p} \tag{15}$$

with $k_3, k_4, k_5 > 0$ such that $k_5 < k_3k_4$.
If $\widetilde{\omega}_b$ converges asymptotically to zero, then $(\widetilde{p},\widetilde{v},\widetilde{a}_b)$ converges asymptotically to zero along the solutions of the position estimation error dynamics (12)*.*

Proof. Appendix B.

Finally, the measured rotation matrix R in (12) and (14) can be replaced by its estimate $\widehat{R}$. However, global asymptotic convergence cannot be achieved anymore, since the observer on $\mathbf{SO}(3)$ is not globally asymptotically stable.

Corollary 2 ***(Nonlinear pose observer)*** *Let*

$$\begin{cases} \frac{d}{dt}\widehat{R} = \widehat{R}S(\omega-\widehat{\omega}_b+\alpha_R), \\ \frac{d}{dt}\widehat{\omega}_b = \alpha_\omega, \end{cases} \tag{16}$$

$$\begin{cases} \frac{d}{dt}\widehat{p} = \widehat{v}+\alpha_p, \\ \frac{d}{dt}\widehat{v} = g_{\mathcal{I}} + \widehat{R}(a-\widehat{a}_b)+\alpha_v, \\ \frac{d}{dt}\widehat{a}_b = \alpha_a, \end{cases} \tag{17}$$

with α_R, α_ω defined by (13)*, and*

$$\alpha_p = k_3\widetilde{p}, \ \alpha_v = k_4\widetilde{p}, \ \alpha_a = -k_5(I_3+\tfrac{1}{k_3}S(\omega-\widehat{\omega}_b))\widehat{R}^T\widetilde{p} \tag{18}$$

Assume that $k_1, \cdots, k_5 > 0$ and $k_5 < k_3k_4$. Then,
1) The origin $(\widetilde{R},\widetilde{\omega}_b,\widetilde{p},\widetilde{v},\widetilde{a}_b) = (I_3,0,0,0,0)$ is a locally exponentially stable equilibrium of the estimation error dynamics.

2) If $\widetilde{R}$ converges asymptotically to I_3, then $(\widetilde{\omega}_b, \widetilde{p}, \widetilde{v}, \widetilde{a}_b)$ converges asymptotically to zero.

Proof. Appendix C.

IV. Implementation issues

While stability of the estimation error is a prerequisite, a good tuning of the innovation gains is also a relevant topic to ensure good response to estimation errors, and respect the sensors characteristics. In IMU-based pose estimation of robotic systems, two dynamics are distinguished: fast dynamics for pose variables and their derivatives, slow dynamics of the gyroscope and accelerometer bias. In this section, we propose a gain tuning strategy for the proposed observer that has a direct interpretation in terms of time-response.

First, consider the attitude observer. Let τ_1, τ_2 denote two settling times with $\tau_1 \ll \tau_2$. The parameter τ_1 denotes a desired settling time for the dynamics of the attitude estimation error dynamics. A typical value (depending of course of the measurements characteristics) is $\tau_1 \leq 1$. As for τ_2, it denotes a desired settling time for the gyroscope bias estimation error. Since this bias varies slowly, a relatively large value of τ_2 can be considered (e.g. $\tau_2 \approx 10$, or even larger). The gains k_1 and k_2 for the attitude estimator are defined as follows:

$$k_1 = 3\tfrac{\tau_1+\tau_2}{\tau_1\tau_2}, \quad k_2 = 9\tfrac{1}{\tau_1\tau_2}. \tag{19}$$

The rationale for this choice is the following. The error system for the attitude estimator can also be written as:

$$\begin{cases} \frac{d}{dt}\widetilde{R} \;=\; -S(R\widetilde{\omega}_b)\widetilde{R} - k_1\widetilde{R}\mathbf{P_a}\big(\widetilde{R}\big), \\ \frac{d}{dt}\widetilde{\omega}_b = k_2\widehat{R}^T\mathbf{vex}\big(\mathbf{P_a}\big(\widetilde{R}\big)\big). \end{cases} \tag{20}$$

In order to simplify the analysis, the gyroscope bias error is expressed in $\{\mathcal{I}\}$, i.e. $\widetilde{\omega}_{\mathcal{I}b} = R\widetilde{\omega}_b$, using (1) and (20) yields

$$\tfrac{d}{dt}\widetilde{\omega}_{\mathcal{I}b} = \tfrac{d}{dt}(R)\widetilde{\omega}_b + k_2\mathbf{vex}\big(\mathbf{P_a}(\widetilde{R})\big).$$

Consider a hover flight situation, i.e. $\frac{d}{dt}R \approx 0,\ \omega_{\mathcal{B}} \approx 0$. Defining $\widetilde{\Theta}$ as any parametrization $\widetilde{R} \approx I_3 + S(\widetilde{\Theta})$ around the identity matrix, from (2), (20), the linearized dynamics of the attitude estimation error dynamics around the equilibrium point $\widetilde{\Theta} = 0$ yields

$$\frac{d}{dt}\begin{bmatrix}\widetilde{\Theta}\\ \widetilde{\omega}_{\mathcal{I}b}\end{bmatrix} = \begin{bmatrix}-k_1 I_3 & -I_3\\ k_2 I_3 & 0\end{bmatrix}\begin{bmatrix}\widetilde{\Theta}\\ \widetilde{\omega}_{\mathcal{I}b}\end{bmatrix}.$$

This system can be decomposed into three independent second-order linear systems:

$$\frac{d}{dt}\begin{bmatrix}\widetilde{\Theta}_i\\ \widetilde{\omega}_i\end{bmatrix} = \begin{bmatrix}-k_1 & -1\\ k_2 & 0\end{bmatrix}\begin{bmatrix}\widetilde{\Theta}_i\\ \widetilde{\omega}_i\end{bmatrix}, \quad (i = 1, 2, 3), \tag{21}$$

and the characteristic polynomial of these systems is

$$\begin{aligned} P(s) = s^2 + k_1 s + k_2 &= s^2 + 3\tfrac{\tau_1+\tau_2}{\tau_1\tau_2}s + \tfrac{9}{\tau_1\tau_2} \\ &= \left(s + \tfrac{3}{\tau_1}\right)\left(s + \tfrac{3}{\tau_2}\right). \end{aligned}$$

Hence, the gain choice (19) yields two real eigenvalues $\lambda_1 = -\frac{3}{\tau_1}, \lambda_2 = -\frac{3}{\tau_2}$. Furthermore, using the variable change (assuming $\tau_1 \neq \tau_2$)

$$\begin{bmatrix}x_1(t)\\ x_2(t)\end{bmatrix} = \begin{bmatrix}\lambda_1 & 1\\ \lambda_2 & 1\end{bmatrix}\begin{bmatrix}\widetilde{\Theta}_i(t)\\ \widetilde{\omega}_i(t)\end{bmatrix}, \tag{22}$$

then Eq. (21) writes

$$\frac{d}{dt}\begin{bmatrix}x_1\\ x_2\end{bmatrix} = \begin{bmatrix}\lambda_1 & 0\\ 0 & \lambda_2\end{bmatrix}\begin{bmatrix}x_1\\ x_2\end{bmatrix}. \tag{23}$$

By using (22) and (23), it is not difficult to obtain the following expression for the solutions of System (21):

$$\widetilde{\Theta}_i(t) = e^{\lambda_1 t}\widetilde{\Theta}_i(0) + \frac{f_{12}(t)}{\lambda_1-\lambda_2}\widetilde{\omega}_i(0) + \frac{\lambda_2 f_{12}(t)}{\lambda_1-\lambda_2}\widetilde{\Theta}_i(0)$$
$$\widetilde{\omega}_i(t) = e^{\lambda_2 t}\widetilde{\omega}_i(0) + \frac{\lambda_1\lambda_2 f_{12}(t)}{\lambda_1-\lambda_2}\widetilde{\Theta}_i(0) + \frac{\lambda_2 f_{12}(t)}{\lambda_1-\lambda_2}\widetilde{\omega}_i(0)$$

with $f_{12}(t) = e^{\lambda_1 t} - e^{\lambda_2 t}$. Therefore the following (partial) dynamics decoupling is obtained:

- Fast exponential decrease of $\widetilde{\Theta}_i(t)$ to zero, corrupted by slowly decreasing terms with small amplitude: $\frac{1}{\lambda_1-\lambda_2}$ and $\frac{\lambda_2}{\lambda_1-\lambda_2}$ tend to zero as $\tau_1 \to 0$ and $\tau_2 \to \infty$.
- Slow exponential decrease of $\widetilde{\omega}_i(t)$ to zero corrupted by slowly decreasing terms with small amplitude.

The same rationale leads to the following definition of the pose estimation observer gains:

$$k_3 = 3\tfrac{\tau_3\tau_4+\tau_3\tau_5+\tau_4\tau_5}{\tau_3\tau_4\tau_5},\ k_4 = 9\tfrac{\tau_3+\tau_4+\tau_5}{\tau_3\tau_4\tau_5},\ k_5 = \tfrac{27}{\tau_3\tau_4\tau_5}. \tag{24}$$

with τ_3, τ_4, and τ_5 different settling times. These gains satisfy the stability conditions of Theorem 1. Choosing $\tau_3, \tau_4 \ll \tau_5$ leads to the same (partial) decoupling of the dynamics of $\widetilde{p}, \widetilde{v}$ on one hand, and $\widetilde{a}_b$ on the other hand.

V. Results

Two simulations are carried out to illustrate the observer's performance and robustness with respect to measurement noise and large initial errors. The first one concerns the evaluation of the nonlinear observer and gain tuning method when facing large initial errors, and the second one consists of a flight simulation with visual feedback. Both simulations were performed using rotational velocity and specific acceleration sampled at a frequency of 100 Hz. The measurement noises considered for the inertial sensors are obtained from a xSens MTi-G unit, presenting variance of $4 \times 10^{-2}\ [\mathrm{rad}]^2$ and $7 \times 10^{-3}\ [\mathrm{m/s^2}]^2$ for rate gyroscopes and accelerometers respectively. To present a measurement noise corrupted by non-Gaussian source, attitude and position are reconstructed by a perspective camera sampling at 10 Hz frequency. The camera is simulated with the following parameters

$$K_f = \begin{bmatrix}1313 & 0 & 512\\ 0 & 1313 & 384\\ 0 & 0 & 1\end{bmatrix}, R_{\mathcal{B}}^{\mathcal{C}} = \begin{bmatrix}1 & 0 & 0\\ 0 & -1 & 0\\ 0 & 0 & -1\end{bmatrix}, p_{\mathcal{B}}^{\mathcal{C}} = 0,$$

with K_f being its calibration matrix, $R_{\mathcal{B}}^{\mathcal{C}}$ and $p_{\mathcal{B}}^{\mathcal{C}}$ the rotation matrix and translational displacement $\{\mathcal{B}\} \to \{\mathcal{C}\}$, where $\{\mathcal{C}\}$ is the reference frame attached to the optical axis of the camera. The visual system is capable of tracking a

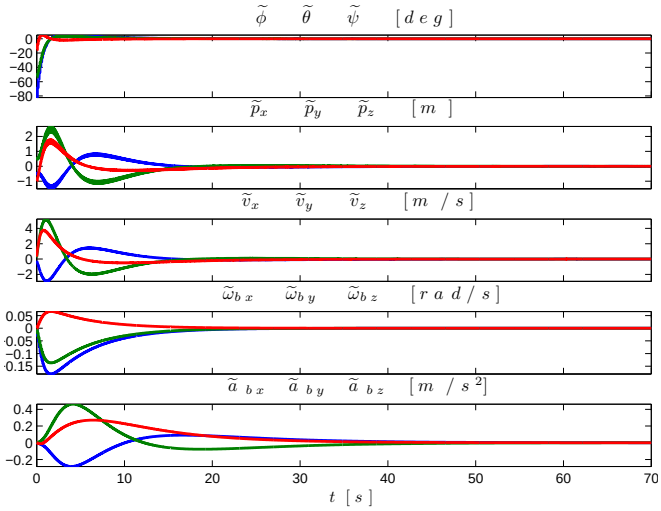

Fig. 1. Simulation for a body at rest. Roll $\widetilde{\phi}$, pitch $\widetilde{\theta}$ and yaw $\widetilde{\psi}$ errors are presented in blue, green, and red respectively. For the other variable $\widetilde{p}$, $\widetilde{v}$, $\widetilde{\omega}_b$, and $\widetilde{a}_b$, the components x , y, z are presented in blue, red, and green respectively. Typical result from repeated simulations.

point, however its projection is corrupted by a Gaussian noise with $\frac{1}{9}$ $[\text{pixel}]^2$ variance for the width and height pixels. To recover the rotation and the translational displacement between two views, the *homography* between a reference and the current image is recovered using the *four point method*. For further information on image formation and pose recovering from two different views the interested reader is conducted to [19]. The observer gains are computed from the aforementioned method given the following settling times τ_1=2 [s], τ_2=15 [s], τ_3=4 [s], τ_4=4 [s], τ_5=25 [s], yielding the gains k_1=1.7, k_2=0.3, k_3=1.62, k_4=0.743, k_5=0.068. The nonlinear observer presented in Corollary 2 is used.

A. Observer convergence from large initial errors

This simulation concerns the convergence of the proposed estimation for large initial errors. The body is at rest with $R(t) = I_3$, $p(t) = [0\ 0\ 1]$, and IMU biases are around 5×10^{-2} $[\text{rad}]$ for gyroscopes and 3×10^{-2} $[\text{m/s}^2]$ for accelerometers. The estimator is initialized with random estimates obtained from zero-mean Gaussian distributions: $\widehat{R}(0) = \exp\{0.999\pi S(u)\}$, where $u \in \mathbb{R}^3$ is a unitary-norm random vector, and $\widehat{p}(0)$, $\widehat{v}(0)$, $\widehat{\omega}_b(0)$, $\widehat{a}_b(0)$ are drawn from zero-mean Gaussian distributions with 3 $[\text{m}]^2$, 1 $[\text{m/s}]^2$, 0.5 $[\text{rad}]^2$ and 0.5 $[\text{m/s}^2]^2$ variance respectively. Fig. 1 depicts the evolution of estimation errors for a typical result from repeated trials. From top to bottom, the results for the attitude error in Euler angles, position, velocity, gyroscope and accelerometer bias errors are presented. Notice the convergence for all the estimates, and that defined settling times correspond to the dominant dynamics for each variable's response. In order to better visualize the convergence of the biases, Fig. 2 presents a closer view for the biases after the settling time has passed. From top to bottom, the results for gyroscope and accelerometer bias are presented. The biases are estimated with a good precision regarding the measurement noises.

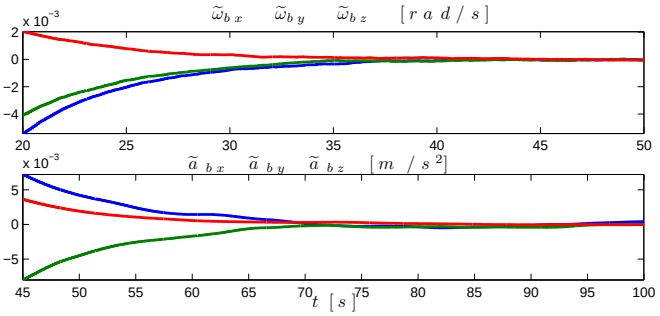

Fig. 2. Closer view on extended time for the visualization of biases error on steady state. Results for components x, y, z are presented in blue, red, and green respectively. Typical result from repeated simulations.

B. On–flight simulation

This simulation aims to evaluate the proposed algorithm in a situation that resembles a drone flight surveillance. Also, the results obtained using the proposed observer are compared to the response provided by the classical EKF written after (6) with its parameters chosen as the noises of the system. The trajectory corresponds to a typical drone mission with take-off, surveillance above a point of interest and landing. The camera observes two square targets, each consisting of four points, with sides 40 $[\text{cm}]$ and 2.4 $[\text{m}]$. This way at least one target can be distinguished during the take-off and landing. The rotational movement is designed in order to keep the image inside the camera's sight. The homography matrix is computed, and after its decomposition and a reference frame change the current rotation and position are obtained. Time varying biases are used to simulate temperature variation, thus increasing the complexity of the simulation. From 0 [s] up to 50 [s], no bias is present. After 50 [s] the biases instantly change to $\omega_b = [0.035, -0.053, 0.018]$ [rad], and $a_b = [-0.3, 0.2, -0.1]$ $[\text{m/s}^2]$ and remain until 100 [s] when they start to change with constant derivative reaching zero at 200 [s], and return with constant derivative until 300 [s] when the values change instantly to their original zero value. For a better visualization of the simulation's dynamics, the reader is directed to the attached video. The associated simulation data are available at `http://www-sop.inria.fr/members/Glauco.Scandaroli`.

A typical result obtained from repeated simulations is presented in Fig. 3. The curves for measured, proposed algorithm, and the EKF estimation errors are depicted in gray, solid blue, and dashed red, respectively. Estimation and measurement errors for the attitude are represented on the top left with Euler angles. Position estimation and measurement errors are depicted on the top right. Gyroscope, and accelerometer biases estimation errors are presented on the bottom left and right. It is visually evident that the resulting noise for attitude and the position measurement are not Gaussian. For the EKF, the attitude is estimated with a good precision until the first bias behavior switch at 50 [s], then non-Gaussian noise and time-varying biases corrupt the estimates. Until the end of the simulation, the biases are well estimated, however roll-pitch angles and estimated position start to present a biased behavior. Also, the yaw

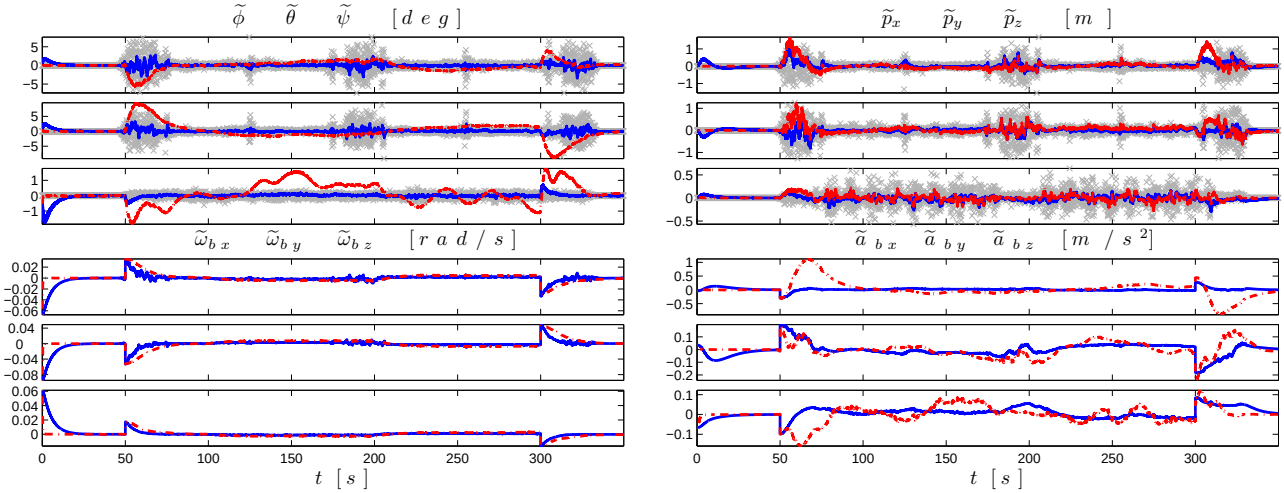

Fig. 3. Simulation for pose estimation during flight surveillance. Comparison of the visual measurement, nonlinear observer, and EKF. Results for visual measurements are presented in gray, nonlinear observer is depicted in solid blue, and EKF in dashed red. Typical result from repeated simulations.

angle does not correspond to the measurements. It could be stated that a 2 [deg] estimation error is not relevant, however considering that the measurements are given within a 0.5 [deg] precision, this error is indeed relevant. Concerning the proposed method, despite the presence of time-varying biases neglected in the observer's design the resulting error presents a smaller variance than the measurement error. Also its precision is better than the EKF. Concerning the gain tuning of the EKF, one may argue that *inflating* model noises might eliminate its convergence problems. This argument is valid, but it also supports the simplicity and effectiveness of the gain tuning method here proposed.

VI. Conclusion and Future Work

This article presents a pose estimation method with online calibration of IMU sensors. A nonlinear observer for concurrent position estimation and accelerometer bias calibration is proposed, together with a global exponential stability proof. A procedure for gain tuning in terms of time-response is also presented. Simulation results endorse the improvement due to the *almost* global stability properties of the nonlinear estimator against locally stable classical estimators. Future work will consist on the evaluation of this approach using real visual-inertial data, and the conduction of a study towards a stochastic evaluation of the innovation gains relating to the measurement noises.

Acknowledgments

The authors would like to thank Rémi Desouche, Ezio Malis, Gregory Chagnet and Daniele Pucci for the useful discussions during the development of this project.

References

[1] J. L. Crassidis, F. L. Markley, and Y. Cheng, "A survey of nonlinear attitude estimation methods," *AIAA Journal of Guidance, Control, and Dynamics*, vol. 30, pp. 12–28, 2007.

[2] B. Bell and F. Cathey, "The iterated Kalman filter update as a Gauss-Newton method," *IEEE Trans. on Automatic Control*, vol. 38, pp. 294–297, 1993.

[3] J. Crassidis, "Sigma-point Kalman filtering for integrated GPS and inertial navigation," *IEEE Trans. on Aerospace and Electronic Systems*, vol. 42, pp. 750–756, 2006.

[4] P. Vernaza and D. Lee, "Rao-Blackwellized particle filtering for 6DOF estimation of attitude and position via GPS and inertial sensors," in *IEEE Intl. Conf. on Robotics and Automation*, 2006, pp. 1571–1578.

[5] A. K. Sanyal, T. Lee, M. Leok, and N. H. McClamroch, "Global optimal attitude estimation using uncertainty ellipsoids," *Systems & Control Letters*, vol. 57, pp. 236–245, 2008.

[6] P. Batista, C. Silvestre, and P. Oliveira, "Sensor-based complementary globally asymptotically stable filters for attitude estimation," in *IEEE Conf. on Decision and Control*, 2009, pp. 7563–7568.

[7] B. Vik and T. Fossen, "A nonlinear observer for GPS and INS integration," in *IEEE Conf. on Decision and Control*, 2001, pp. 2956–2961.

[8] J. Thienel and R. Sanner, "A coupled nonlinear spacecraft attitude controller and observer with an unknown constant gyro bias and gyro noise," *IEEE Trans. on Automatic Control*, vol. 48, pp. 2011–2015, 2003.

[9] M.-D. Hua, "Attitude observers for accelerated rigid bodies based on GPS and INS measurements," in *IEEE Conf. on Decision and Control*, 2009, pp. 8071–8076.

[10] R. Mahony, T. Hamel, and J.-M. Pflimlin, "Nonlinear complementary filters on the special orthogonal group," *IEEE Trans. on Automatic Control*, vol. 53, pp. 1203–1218, 2008.

[11] S. Bonnabel, P. Martin, and P. Rouchon, "Symmetry-preserving observers," *IEEE Trans. on Automatic Control*, vol. 53, pp. 2514–2526, 2008.

[12] P. Martin and E. Salaun, "An invariant observer for earth-velocity-aided attitude heading reference systems," in *IFAC World Conf.*, 2008, pp. 9857–9864.

[13] H. Rehbinder and B. Ghosh, "Pose estimation using line-based dynamic vision and inertial sensors," *IEEE Trans. on Automatic Control*, vol. 48, pp. 186–199, 2003.

[14] G. Baldwin, R. Mahony, and J. Trumpf, "A nonlinear observer for 6 DOF pose estimation from inertial and bearing measurements," in *IEEE Intl. Conf. on Robotics and Automation*, 2009, pp. 2237–2242.

[15] J. Vasconcelos, C. Silvestre, and P. Oliveira, "A nonlinear GPS/IMU based observer for rigid body attitude and position estimation," in *IEEE Conf. on Decision and Control*, 2008, pp. 1255–1260.

[16] T. Cheviron, T. Hamel, R. Mahony, and G. Baldwin, "Robust nonlinear fusion of inertial and visual data for position, velocity and attitude estimation of UAV," in *IEEE Intl. Conf. on Robotics and Automation*, 2007, pp. 2010–2016.

[17] M. D. Shuster, "A survey of attitude representations," *The Journal of the Astronautical Sciences*, vol. 41, pp. 439–517, 1993.

[18] S. Benhimane and E. Malis, "Homography-based 2D visual tracking and servoing," *Intl. Journal of Robotics Research*, vol. 26, pp. 661–676, 2007.

[19] Y. Ma, S. Soatto, J. Kosecka, and S. S. Sastry, *An Invitation to 3-D Vision: From Images to Geometric Models*. SpringerVerlag, 2003.

APPENDIX

A. Proof of Theorem 1

From (12) and (14), pose estimation error dynamics yields

$$\begin{cases} \frac{d}{dt}\widetilde{p} &= \widetilde{v} - k_3\widetilde{p}, \\ \frac{d}{dt}\widetilde{v} &= -R\widetilde{a}_b - k_4\widetilde{p}, \\ \frac{d}{dt}\widetilde{a}_b &= k_5\big(I_3 + \frac{1}{k_3}S(\omega_{\mathcal{B}})\big)R^T\widetilde{p}. \end{cases} \tag{25}$$

Consider the following variable change

$$\gamma = R\widetilde{a}_b + \tfrac{k_5}{k_3}\widetilde{p}, \tag{26}$$

In the coordinates $(\widetilde{p}, \widetilde{v}, \gamma)$, System (25) is thus given by

$$\begin{cases} \frac{d}{dt}\widetilde{p} = \widetilde{v} - k_3\widetilde{p}, \\ \frac{d}{dt}\widetilde{v} = -\gamma - (k_4 - \frac{k_5}{k_3})\widetilde{p}, \\ \frac{d}{dt}\gamma = S(R\omega_{\mathcal{B}})\gamma + \frac{k_5}{k_3}\widetilde{v}. \end{cases} \tag{27}$$

Define the following candidate Lyapunov function:

$$\mathcal{W}_t = \tfrac{1}{2}\left(k_4 - \tfrac{k_5}{k_3}\right)|\widetilde{p}|^2 + \tfrac{1}{2}|\widetilde{v}|^2 + \tfrac{1}{2}\tfrac{k_3}{k_5}|\gamma|^2, \tag{28}$$

and note that $\mathcal{W}_t$ is positive definite due to the assumption $k_3, k_4, k_5 > 0$ and $k_5 < k_3k_4$. Along the solutions of (27),

$$\begin{aligned} \tfrac{d}{dt}\mathcal{W}_t = &\left(k_4 - \tfrac{k_5}{k_3}\right)\widetilde{p}^T(\widetilde{v} - k_3\widetilde{p}) - \widetilde{v}^T\left(\gamma + \left(k_4 - \tfrac{k_5}{k_3}\right)\widetilde{p}\right) \\ &+ \tfrac{k_3}{k_5}\gamma^T\left(S(R\omega_{\mathcal{B}})\gamma + \tfrac{k_5}{k_3}\widetilde{v}\right), \\ = &-k_3\left(k_4 - \tfrac{k_5}{k_3}\right)|\widetilde{p}|^2 \leq 0 \end{aligned} \tag{29}$$

By using Barbalat's Lemma, and Assumption 1, it is not very difficult from here to prove that $(\widetilde{p}, \widetilde{v}, \gamma) = (0, 0, 0)$ is a globally asymptotically stable equilibrium point. However, in order to establish *exponential* stability, it is proceeded differently by modifying $\mathcal{W}_t$ so as to obtain a strict Lyapunov function. Let $\mathcal{W} = \mathcal{W}_t - \epsilon\widetilde{v}^T(\widetilde{p} - \delta\gamma)$ with $\delta \in (0, 1)$ and $\epsilon > 0$ some constants which will be specified further on. Due to the condition $\delta \in (0, 1)$ and the fact that $\mathcal{W}_t$ is positive definite, it is clear that $\mathcal{W}$ is also positive definite for $\epsilon > 0$ "small enough". Let $\overline{k}_4 = (k_4 - \frac{k_5}{k_3})$ and recall that $\overline{k}_4 > 0$. It follows from (29) that along the solutions of System (27),

$$\begin{aligned} \tfrac{d}{dt}\mathcal{W} = &-\overline{k}_4(k_3 - \epsilon)|\widetilde{p}|^2 \\ &- \epsilon\left(\delta|\gamma|^2 + (1 - \delta\tfrac{k_5}{k_3})|\widetilde{v}|^2 - \delta\widetilde{v}^T S(R\omega_{\mathcal{B}})\gamma\right) \\ &+ \epsilon\widetilde{p}^T\left((1 - \delta\overline{k}_4)\gamma + k_3\widetilde{v}\right) \end{aligned} \tag{30}$$

Consider the term

$$L_2 = \delta|\gamma|^2 + (1 - \delta\tfrac{k_5}{k_3})|\widetilde{v}|^2 - \delta\widetilde{v}^T S(R\omega_{\mathcal{B}})\gamma$$

in the second line of (30). From Assumption 1 it follows that

$$L_2 \geq \delta|\gamma|^2 + (1 - \delta\tfrac{k_5}{k_3})|\widetilde{v}|^2 - \delta\overline{c}_\omega|\widetilde{v}||\gamma|.$$

Therefore, with $\delta \in (0, \min(1, \frac{k_3}{k_5}))$ and $\delta^2\overline{c}_\omega^2 < 4\delta(1 - \delta\frac{k_5}{k_3})$, L_2 is a positive definite function of $|\gamma|$, and $|\widetilde{v}|$. Clearly, there exist values of δ which satisfy the above condition. By choosing such a value δ, from (30), it can be deduced that for some constant $\delta' > 0$ independent of ϵ,

$$\begin{aligned} \tfrac{d}{dt}\mathcal{W} \leq &-\overline{k}_4(k_3 - \epsilon)|\widetilde{p}|^2 - \epsilon\delta'\left(|\gamma|^2 + |\widetilde{v}|^2\right) \\ &+ \epsilon\widetilde{p}^T\left((1 - \delta\overline{k}_4)\gamma + k_3\widetilde{v}\right) \end{aligned} \tag{31}$$

Using the fact that

$$\begin{aligned} \left|\epsilon\widetilde{p}^T\left((1 - \delta\overline{k}_4)\gamma + k_3\widetilde{v}\right)\right| &= \left|\epsilon^{\frac{1}{4}}\widetilde{p}^T\epsilon^{\frac{3}{4}}\left((1 - \delta\overline{k}_4)\gamma + k_3\widetilde{v}\right)\right| \\ &\leq \frac{1}{2}\left(\sqrt{\epsilon}|\widetilde{p}|^2 + \epsilon^{\frac{3}{2}}|(1 - \delta\overline{k}_4)\gamma + k_3\widetilde{v}|^2\right), \end{aligned}$$

it is straightforward to verify from (31) that there exists $\epsilon_0 > 0$ such that, for any $\epsilon \in (0, \epsilon_0)$,

$$\tfrac{d}{dt}\mathcal{W} \leq -\eta(\epsilon)\mathcal{W}, \quad \eta(\epsilon) > 0. \tag{32}$$

Since $\mathcal{W}$ is definite positive function for $\epsilon > 0$ small enough, this concludes the proof of global exponential stability of the origin of System (27). Considering the variable transformation (26), it is concluded that the origin of System (25) is also globally exponentially stable. This also follows from the fact that the function $\overline{\mathcal{W}}$ defined by $\overline{\mathcal{W}}(\widetilde{p}, \widetilde{v}, \widetilde{a}_b) = \mathcal{W}(\widetilde{p}, \widetilde{v}, \gamma)$ satisfies inequality (32) along the solutions of System (25).

B. Proof of Corollary 1

The dynamics of the position estimation error (12) can be written as

$$\dot{Y} = A(t)Y + g_1(Y, \widetilde{\omega}_b, t) \tag{33}$$

with $Y = (\widetilde{p}, \widetilde{v}, \widetilde{a}_b)$, $A(t)$ the right-hand side of System (25), and $g_1(Y, \widetilde{\omega}_b, t)$ a "perturbation term" such that

$$|g_1(Y, \widetilde{\omega}_b, t)| \leq c|Y||\widetilde{\omega}_b| \tag{34}$$

for some constant c. This readily implies that the solutions of the system are well defined for all time. From Section A of this appendix, there exists a quadratic Lyapunov function $\overline{\mathcal{W}}$ such that, along the solution of $\dot{Y} = A(t)Y$,

$$\tfrac{d}{dt}\overline{\mathcal{W}} \leq -\eta\overline{\mathcal{W}}, \quad \eta > 0 \tag{35}$$

Furthermore, it is considered that $\widetilde{\omega}_b(t)$ converges asymptotically to zero regardless of the initial conditions. Then, it is deduced from (34) and (35) that, along any solution of System (33), there exists $T \geq 0$ such that for $t \geq T$, $\frac{d}{dt}\overline{\mathcal{W}} \leq -\frac{1}{2}\eta\overline{\mathcal{W}}$. Convergence to zero of Y readily follows from this inequality.

C. Proof of Corollary 2

The dynamics of the position estimation error (12) can be written as

$$\begin{cases} \dot{X} = f_0(X, t) \\ \dot{Y} = A(t)Y + g_2(X, Y, t) \end{cases} \tag{36}$$

with $X = (\widetilde{R}, \widetilde{\omega}_b)$, $Y = (\widetilde{p}, \widetilde{v}, \widetilde{a}_b)$, $f_0(X, t)$, $A(t)$ the right-hand side of System (25), and $g_2(X, Y, t)$ a "perturbation term" such that

$$|g_2(X, Y, t)| \leq c|X|(1 + |X|)|Y| \tag{37}$$

for some constant c. From [10], there exists a quadratic Lyapunov function $\mathcal{U}$ for the system $\dot{X} = f_0(X, t)$ such that, in a neighborhood of $X = (I_3, 0)$, $\frac{d}{dt}\mathcal{U} \leq -\eta'\mathcal{U}$ with $\eta' > 0$. By setting $\mathcal{V} = U + \overline{\mathcal{W}}$, it is verified from (36), and (37) that in a neighborhood of $(X, Y) = \big((I_3, 0), 0\big)$, $\frac{d}{dt}\mathcal{V} = -\eta''\mathcal{V}$ with $n'' > 0$. This shows Property 1) of Corollary 2. The proof of Property 2) is similar to Corollary 1.